Journal of King Saud University – Computer and Information Sciences 34 (2022) 8955–8971

HOSTED BY

Contents lists available at ScienceDirect

Journal of King Saud University – Computer and Information Sciences

journal homepage: www.sciencedirect.com

Combined economic emission dispatch in hybrid power systems using competitive swarm optimization

Prabhujit Mohapatra

Department of Mathematics, School of Advanced Sciences, Vellore Institute of Technology, Vellore 632014, India

ARTICLE INFO

Article history:
Received 10 June 2022
Revised 26 July 2022
Accepted 18 August 2022
Available online 28 August 2022

Keywords:
Hybrid power system problem
Emission
Renewable energies
Competitive swarm optimization

ABSTRACT

In last few decades, the emission of greenhouse gasses has exponentially increased due to large production of electric power energy from conventional fossil fuels to pose critical environmental challenges. The renewable energies (REs) are establishing themselves as key technologies for reduction of carbon emissions, in addition to low cost and high efficiency. However, the operational limits and the power generation procedures of the renewable energies invite immense challenges. The uncertainty in production with precise and error free approximation make it very complicated. Hence, an effective approach with methodical organization of the renewable energies are the need of the hour for reliable and safe system. In this study, an IEEE 30-bus hybrid power system (HPS) problem consisting of conventional thermal generators and green energies like wind generators and solar photovoltaic are considered to become environmentally and economically capable than the existing ones. Several measures like penalty cost and reserve cost have been considered in this present study for addressing the uncertainty issues underestimation and overestimation respectively. Further, three hybrid configurations such as thermal-solar (TS), thermal-wind (TW) and thermal-wind-solar (TWS) are proposed to perform the cost effective analysis. The adopted hybrid power system is extremely complex and non-linear optimization problem. Hence, a recently proposed evolutionary algorithm namely competitive swarm optimization (CSO) algorithm is implemented to discover the optimum result for the variety goals like minimum production cost, carbon emission, voltage variation and loss of the power. The performance of CSO algorithm is compared with several state-of-the-art *meta*-heuristic algorithms such GA, PSO, CSA, ABC, and SHADE-SF. The extraordinary outcomes achieved in this work illustrate that the CSO method can successfully be applied to handle the complex, non-convex and non-linear hybrid power system problems.

1. Introduction

With the increased demand in electricity production, the environmental consequences pose a great challenge to affect the world economy. The fertile agricultural land will experience drought and warmer climate, affecting its crop harvests to drop. The fall in agricultural land's crop harvest is a long-lasting damage to the economy of a country. The infrastructures will get damaged by floods, cyclones and hurricanes, causing to spend billions of dollars to rebuild. These situations could hit to G.D.P in coming days. As per the recent 2017 report (IEA, 2019) of the International Energy Agency, the total primary energy supply of the world has reached 162,494 terawatt-hour (*TWh*) or equivalent to 13,972 millions of tons of oil equivalent (*Mtoe*) and out of which the fossil energy accounts for 80 % of it. The overall major energy source in 1971 and 2017 is represented in Fig. 1. The primary reason for the huge demand in fossil energy is due to the rapid industrialization, exponential population growth and advancement in technologies. As a consequence, the environmental condition starts to decorate with increased emission of greenhouse gases. This poses a great challenge to consider other cleaner sources of energies with cost effective way. Hence, the renewable energies through hybrid power systems have received the unparalleled attention in recent times (Destek and Sinha, 2020; Li et al., 2020; Li et al., 2020) to satisfy the demand of clean energies with least cost.

The classical hybrid power system model is designed to allocate the requisite power from the conventional thermal generators to

E-mail address: prabhujit.mohapatra@vit.ac.in
Peer review under responsibility of King Saud University.

Production and hosting by Elsevier

https://doi.org/10.1016/j.jksuci.2022.08.022

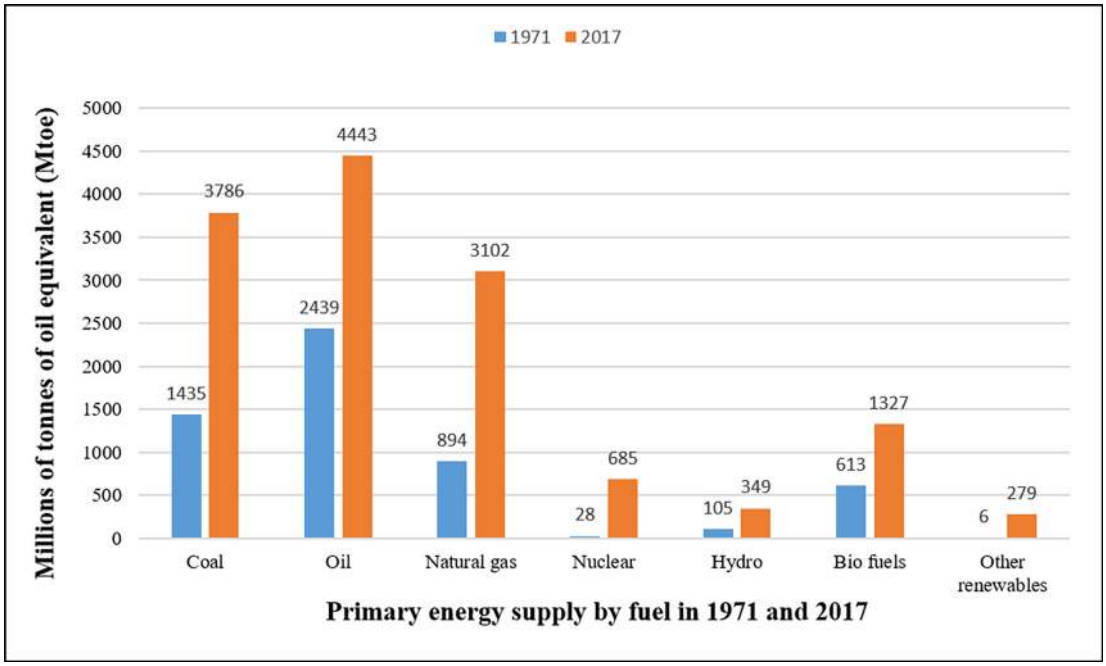

Fig. 1. Comparison of fuel supply in 1971 and 2017.

reduce the whole operating cost irrespective of generated emission while fulfilling all the limitations (Mahor et al., 2009). The primary objectives of these research works are to increase the efficiency of the projected algorithms in considering different complex goals like multi-fuel scenario, valve point effect (Chaib et al., 2016; Bouchekara et al., 2016) and convergence speed (Mohamed et al., 2017). However, the production of energy from the traditional fossil fuel releases major greenhouse gases such as SO_x, CO_x and NO_2 which affect not only the humans but also other animals and plants. The annual change in CO2 emissions in 2000–2018 (IEA, 2019) is presented in Fig. 2. From this figure it can be established that in the period 2010–2016 the average carbon emissions has followed annual drop of 1 % but in 2018 emissions started to grow again at 0.5 %. Despite the increase in average carbon emissions in 2018, the countries like the United States, Canada and Korea, several countries exhibited overall drops, most remarkably by Japan, Germany and France (IEA, 2019).

Therefore, the economic load dispatch (ELD) problem has been passed by the Clean Air Organization to contain the greenhouse gasses since 1990 (H.R.,1990). The outline formed by United Nations on Climate Change (Lu et al., 2010) has proposed to impose the carbon tax in order to tackle the greenhouse emissions by

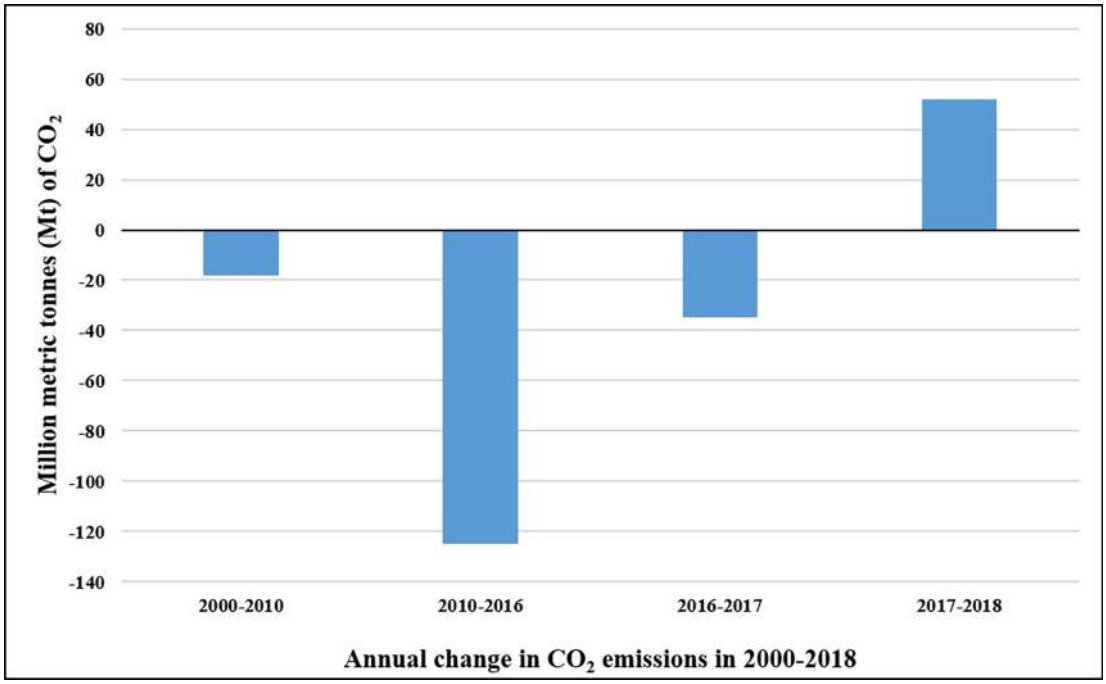

Fig. 2. Scenario of CO_2 emissions in between 2000 and 2018.

increasing the operational cost. However, the previous works only emphasize to decrease the level of pollutants in fossil fuel by improving the dispatch strategies. But now a days the renewable energies such as wind and solar have gained wide recognition due to their zero emission and low fuel cost advantages. Hence, the CEED model with wind power and solar power is being incorporated by the researchers across the world (Panda et al., 2020) to minimize emission as well as the cost. The first CEED model incorporating wind power was proposed in (Hetzer et al., 2008) to analyze the effect of optimal solutions. The stochastic model of wind generation was introduced in (Jabr and Pal, 2009) for realistic presentation of hybrid power system. The constraints on the generation of wind power energy are considered in (Liu and Xu, 2010; Liu, 2011). Subsequently, the massive wind power generating systems was proposed as dynamic economic dispatch (DED) model in (Wei et al., 2011). The remote hybrid power system with solar photovoltaic and diesel generator was reflected in (Henerica et al., 2015). The propelled hydro generator was presented in (Kanzumba, 2016) as an alternative form of storage to the hybrid power system consisting solar photovoltaic, wind and diesel generators. The grid adjustment of wind and solar photovoltaic power is complex due to their uncertainty nature. The probability distribution of the renewable energies wind and solar photovoltaic follow the Weibull and lognormal density functions respectively (Chang, 2010; International Electrotechnical Commission., 2005). Occasionally, the power output from these renewable energies bears the penalty cost for underestimating the scheduled power by producing surplus energy than required. On contrary to this, sometimes they produce less energy than the scheduled power to create the overestimation scenario forcing the uses of expensive reserved energy. The uncertainty nature of the renewable energies displays serious challenges for the execution of the power system. The uncertainty in production with precise and error free approximation make the renewable energies very complicated. By considering the present scenario, it can be established that the modifications in prevailing sharing policies to minimize mutually the fuel price and amount of pollutants are the critical research topic. Therefore, with increasing demand in energy consumptions and consciousness of eco-friendly effects, great effectiveness deployment for renewable energies like wind and solar have paid more attention throughout the world. In ELD problems, when the environmental concerns are attached then they are popularly known as combined economic emission power dispatch problems (CEED). The solution of CEED (Wolpert and Macready, 1997) problems focuses to generate the powers at lowest cost with least emission effect. Several classical optimization algorithms such as linear programming (Nanda et al., 1988); lagrangian method (El-Keib et al., 1994), analytical methods (Anantasate and Bhasaputra, 2011) and Newton-Raphson method (Chen and Chen, 2003) have been deployed to discover the quality solution of the real-world CEED problems. But, these methods fail to handle efficiently due to the non-smooth and non-convex properties of the CEED problems.

Hence, the nature inspired *meta*-heuristic algorithms are widely applied in handling different real life complex problems for having the capabilities in resolving the non-linear situations. Some of the popular *meta*-heuristic algorithms such as GA (Ganjefar and Tofighi, 2011), PSO (Abdullah et al., 2013), DE (Peng et al., 2012), ACO (Karakonstantis and Vlachos, 2018), BFA (Hota et al., 2010), CSA (Hassanien et al., 2018), ABC (Adaryani and Karami, 2013), FPA (Harifi et al., 2020) and GPC (Yang, 2012) have been extensively examined in solving the CEED problems. However, the 'No Free Lunch Theorem' [48] cites that no evolutionary *meta*-heuristic optimization algorithm can solve all the real life engineering problems efficiently. Hence, there is a need to propose new *meta*-heuristics subsequently to handle the new complex problems.

Henceforth, at first, this paper focuses an effective approach with methodical accomplishment of the renewable energies for reliable and safe system. Several measures like reserve cost and penalty cost have to be taken into account to regulate the uncertain productions. Secondly, the paper focuses for the proper integration of conventional thermal and renewable energies. The appropriate penetration of renewable energies may able to reduce the generation cost. Finally, the work attempts producing the ideal power schedule amid the generators for minimizing the generating cost, carbon emission, transmission power loss and deviation of voltage by implementation of a novel heuristic evolutionary algorithm. In order to promote the renewable energy sources, carbon tax (Yao et al., 2012; Roy et al., 2010) is imposed on each unit of released poisonous gasses to represent emission in terms of cost. The novel competitive swarm optimization algorithm (CSO) (Cheng and Jin, 2014) is deployed to find the solution of the adopted problem. The CSO being a nature inspired algorithm neither follows the particle best position and global best position to modernize the swarm members. Instead, the algorithm produces a pair wise competitive mechanism to apprise the position of the particles. The results of the CSO algorithm is analyzed with several state-of-the-art algorithms (Ganjefar and Tofighi, 2011; Abdullah et al., 2013; Peng et al., 2012; Karakonstantis and Vlachos, 2018; Hota et al., 2010; Hassanien et al., 2018; Adaryani and Karami, 2013; Harifi et al., 2020; Yang, 2012; Biswas et al., 2017) to provide accurate and fast convergence solution of the non-linear constrained *HPS* problem.

The remainder of this paper is presented as following. The modelling of the constrained hybrid power system problem and the uncertain behavior of the renewable energies have been addressed in Section 2. The objectives and case studies of the HPS are established in section 3. The description and implementation of the CSO algorithm are explained in section 4. The section 5 focus with parameter setting and analysis of the experimental results. In this part, firstly-three different hybrid configurations such as TS, TW and TWS have been proposed to produce the cost effective analysis. Secondly, the CSO algorithm has been implemented to the best cost effective configuration to report the optimum solution for all the objectives and case studies. Lastly, the conclusion is provided in section 6.

2. Mathematical formulation

Here, a 30-bus IEEE hybrid power system (*HPS*) problem comprises of thermal, wind and solar generators is adopted for analysis. As the behavior of wind and solar generators is intermittent in nature, hence the hybrid power system problem is non-convex, non-linear and irregular. These complicated nature of the HPS restrain the system operator from the ultimate consumption of the green energies. Therefore, the uncertainty of power creation in renewable energies must be adjusted from other resources to balance the load demand and generation. To confirm the ultimate exploitation of green energies, appropriate scheduling and allocation between other resources are required. The graphical illustration of a sample *HPS* is displayed in Fig. 3 and the required parameters are listed in Table 1.

2.1. Thermal generators fuel cost

Thermal generators depend on traditional energy sources such as natural gas, coal, petrol and diesel. The produced powers (MW) of these generators directly depend on the amount of fuel

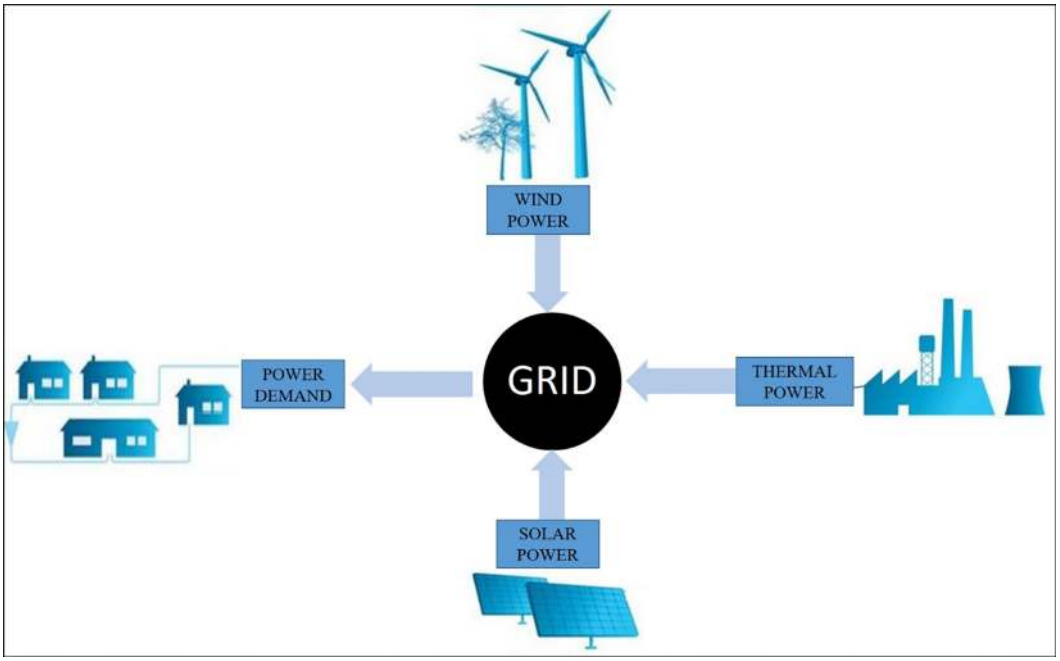

Fig. 3. Graphical illustration of a hybrid power system (*HPS*).

Table 1
Parameters of the adopted 30-bus IEEE system.

Entities	Size	Particulars
No. of buses	30	Alsac and Stott, 1974
No. of branches	41	
No. of thermal generators	03	*TG*1, *TG*2 and *TG*3 are connected to bus no. 1, 2 and 8 respectively.
No. of wind generators	02	Wind generators *WG*1 and *WG*2 are connected at bus no. 5 and 11 respectively.
No. of solar photovoltaic	01	Solar photovoltaic *SPV* is connected at bus no. 13.
No. of control variables	11	Real power for 2 thermals (*TG*2 and *TG*3), 2 winds (*WG*1 and *WG*2), 1 solar generator (*SPV*) and voltage for all 6 connected buses.
Connected load capacity	–	283.4 MW and 126.4 *MVAr*
load bus voltage range	24	$[0.95 - 1.05]p.u.$

cost. Hence, the relationship among fuel cost ($/h$) and produced power (MW) can be estimated by a quadratic equation defined as:

$$Fuel\ cost_{TG} = \sum_{i=1}^{N_{TG}} \alpha_i + \beta_i P_{TGi} + \gamma_i P_{TGi}^2 \tag{1}$$

where, P_{TGi} is power output and α_i, β_i and γ_i are the suitable coefficients of the i^{th} thermal generating unit. N_{TG} represents the total thermal generators. The effect of valve-point has to be reflected for better convincing and accurate projection of cost of the fuel. The turbines with multi-valve in thermal generators show a larger difference in fuel cost (Bouchekara et al., 2016). Hence, the consequence of multi-valve turbines is added to the eqn. (1) to obtain an updated total cost of thermal generators as:

$$Valve\ Point\ Effect = \sum_{i=1}^{N_{TG}} \alpha_i + \beta_i P_{TGi} + \gamma_i P_{TGi}^2 + \left| r_i \times \sin\left(s_i \times \left(P_{TGi}^{min} - P_{TGi}\right)\right)\right| \tag{2}$$

where, r_i and s_i are the valve-point coefficients and P_{TGi}^{min} is the least power production capacity of the i^{th} thermal unit. The required parameters of all the thermal power generators are noted in Table 2.

2.2. Direct cost of renewable energies

The solar photovoltaic and wind generators do not need fossil fuel and are very different from the traditional thermal generators. However, the wind and solar photovoltaic plants pay a cost proportionate to the scheduled power output. This cost is formed from the accumulation of initial layout, maintenance and renewal cost (Chen et al., 2006). Hence, the cost for the k^{th} wind power is exhibited in terms of power output as:

$$Direct\ cost_{WGk}(P_{WGk}) = u_k P_{WGk} \tag{3}$$

where, u_k is the cost coefficient of the connected k^{th} wind turbine and P_{WGk} is the expected power from the specified generator. Likewise, the cost for the l^{th} solar photovoltaic is given as:

$$Direct\ cost_{SPVl}(P_{SPVl}) = v_l P_{SPVl} \tag{4}$$

where, v_l is the cost coefficient of the related l^{th} solar PV plant and P_{SPVl} is the power of the generator.

2.3. Uncertainty cost of renewable energies

The renewable energies are unpredictable in nature. Sometimes they fail to produce the required power whereas, other times they produce more than the required amount. The first situation is called an overestimation situation from the unpredictable energy sources. Therefore, there is need of to have separate energy reserve to match the requirement. The cost of engaging the reserve generators to fulfill the overestimated sum is called as reserve cost (Panda and Tripathy, 2015). Hence, the reserve cost for the wind generators and solar photovoltaic generators are provided as follows.

Reserve cost for overestimation of k^{th} wind generator is:

Table 2
The thermal generators coefficients for the considered problem.

Power generator	Load bus	α	β	γ	r	s	a	b	c	δ	θ
$TG1$	1	0	2	0.0037	18	0.037	4.091	−5.554	6.49	0.0002	6.667
$TG2$	2	0	1.75	0.0175	16	0.038	2.543	−6.047	5.638	0.0005	3.333
$TG3$	8	0	3.25	0.0083	12	0.045	5.326	−3.55	3.38	0.002	2

$$Reserve\ cost_{WGk}(P_{WGk}-P_{WGak}) = K_{RWGk}(P_{WGk}-P_{WGak}) = K_{RWGk} \times \int_0^{P_{WGk}} (P_{WGk}-p_{WGk}) f_{WG}(p_{WGk}) dp_{WGk} \quad (5)$$

The solar photovoltaic follows lognormal *PDF* (Shi et al., 2012) which is very different from Weibull *PDF* of the wind generators. The parameters of these probability density functions are listed in Table 3. The reserve cost for the solar photovoltaic is made on the basis of the definitions provided in Mohapatra et al. (2019). Therefore, the reserve cost for overestimation of l^{th} solar photovoltaic is:

$$Reserve\ cost_{SPVl}(P_{SPVl}-P_{SPVal}) = K_{RSPVl}(P_{SPVl}-P_{SPVal})$$

$$= K_{RSPVl} * f_{SPV}(P_{SPVal} < P_{SPVl}) * [P_{SPVl} - E(P_{SPVal} < P_{SPVl})] \quad (6)$$

where, K_{RWGk} and K_{RSPVl} are the reserve cost coefficients of the k^{th} and l^{th} wind and solar plant respectively. The parameters P_{WGak} and P_{SPVal} are the actual available power from the respective plants. The density functions for the wind and solar are given as f_{WG} and f_{SPV} respectively. The probability function $f_{SPV}(P_{SPVal} < P_{SPVl})$ represents the chances of shortage occurrence than the scheduled power. The parameter $E(P_{SPVal} < P_{SPVl})$ represents the expectation of available power below the scheduled power for the solar generator. The calculation of probability density function for the wind and solar energies is adopted from the available research work (Shi et al., 2012).

In contradiction to the power overestimation situation, there exists another case of power underestimation. In this case, the renewable energies produce higher power output than the estimated amount. Therefore, it is required to utilize the surplus power of the renewable energies by dropping the power production from thermal generators. The cost functions for the calculation of penalties have been added in both wind and solar models to balance the surplus amount as follows.

Penalty cost for underestimation of k^{th} wind generator is:

$$Penalty\ cost_{WGk}(P_{WGak}-P_{WGk}) = K_{PWGk}(P_{WGak}-P_{WGk})$$

$$= K_{PWGk}\int_{P_{WGk}}^{P_{WGrk}} (p_{WGk}-P_{WGk}) f_{WG}(p_{WGk}) dp_{WGk} \quad (7)$$

Penalty cost for underestimation of l^{th} solar photovoltaic is:

$$Penalty\ cost_{SPVl}(P_{SPVal}-P_{SPVl}) = K_{PSPVl}(P_{SPVal}-P_{SPVl})$$

$$= K_{PSPVl} * f_{SPV}(P_{SPVal} > P_{SPVl}) * [E(P_{SPVal} > P_{SPVl})] - P_{SPVl} \quad (8)$$

where, K_{PWGk} and K_{PSPVl} are the penalty cost coefficients of the k^{th} and l^{th} wind plant and solar plant respectively. The parameters P_{WGak} and P_{SPVal} are the actual available power from the respective plants. The notation P_{WGrk} presents the rated power output of the k^{th} wind firm. The probability density function $f_{SPV}(P_{SPVal} > P_{SPVl})$ represents the surplus occurrence chances than the scheduled power. The parameter $E(P_{SPVal} > P_{SPVl})$ represents the expectation of available power above the scheduled power for the solar generator.

2.4. Emission cost

It is established that power generated from traditional thermal energies like coal, petrol, gas and diesel releases harmful gases such as SO_x and NO_x into the atmosphere. The release of the toxic gases escalates with the rise in produced power from the thermal generators. Hence, the emission is calculated in tonnes per hour (ton/h) by the following equation:

$$Emission = \sum_{i=1}^{N_{TG}} \left[\left(a_i + b_i P_{TGi} + c_i P_{TGi}^2 \right) \times 0.01 + \delta_i e^{(\theta_i P_{TGi})} \right] \quad (9)$$

where, a_i, b_i, c_i, δ_i and θ_i are the emission coefficients of the i^{th} thermal generator.

In recent times, several nations are placing immense burden on the whole energy division to cut carbon emissions because of global warming. In order to promote the green energy sources like hydro power, wind power and solar power, the carbon tax factor $(Carbon_{tax})$ is levied on each unit of released poisonous gasses to represent emission with respect to cost. Hence, the emission cost $(/h)$ is given as:

$$Emissioncost = Carbon_{tax} * Emission \quad (10)$$

2.5. Power loss with voltage deviation

Another significant factors in HPS models are the actual network power loss and deviation of voltage. Because of the inherent resistance of the lines, the power loss in the system is inevitable. The power loss is estimated as:

$$Power\ loss = \sum_{j=1}^{nl} \sum_{k \neq i}^{nl} G_{jk} V_j^2 + V_k^2 - 2V_j V_k cos(\delta_{jk}) \quad (11)$$

where, $\delta_{jk} = \delta_j - \delta_k$, is the voltage angles change between bus j and bus k. G_{jk} is the transmission conductance and nl is the overall lines.

Table 3
The strictures of the wind and solar probability density functions.

Wind generators					Solar photovoltaic		
Wind generators	Number of turbines	Rated power (MW)	Parameters of Weibull *PDF*	Weibull mean (m/s)	Rated power (MW)	Parameters of Lognormal	Lognormal mean
$WG1$ connected to bus 5	25	75	9 and 2	7.976	50 connected to bus 13	Mean is 6 and Std. is 0.6	$483 W/m^2$
$WG2$ connected to bus 11	20	60	10 and 2	8.862			

In the model, voltage deviation is the degree of quality of voltage. The voltage deviation parameter is considered as accumulative variation of voltage of entire load buses. It may be presented as.

$$Voltage\ deviation = \left(\sum_{p=1}^{NL} |V_{L_p} - 1|\right) \tag{12}$$

where, NL is the overall number of load buses and V_{L_p} is the voltage at loss bus respectively.

2.6. Equality constraints

In hybrid power system problem, the total produced active power and reactive power should be equivalent to the total demand and losses (Biswas et al., 2017). Hence, the power equilibrium equations form the balanced constraints of the system which are shown in eqns. (13) and (14) respectively.

$$P_{Gj} - P_{Dj} - V_j \sum_{k=1}^{Nbus} V_k \left[G_{jk}\cos(\delta_{jk}) + B_{jk}\sin(\delta_{jk})\right] = 0 \forall j \in Nbus \tag{13}$$

$$Q_{Gj} - Q_{Dj} - V_j \sum_{k=1}^{Nbus} V_k \left[G_{jk}\sin(\delta_{jk}) - B_{jk}\cos(\delta_{jk})\right] = 0 \forall j \in Nbus \tag{14}$$

where, $Nbus$ counts the overall number of buses. Similarly, the active load and reactive load demands at bus j is given by P_{Dj} and Q_{Dj} respectively. Similarly, the active power generations and reactive power generations from bus j are given by P_{Gj} and Q_{Gj} respectively. The other parameters G_{jk} and B_{jk} represent the transmission conductance and susceptance between bus j and bus k correspondingly.

2.7. Inequality constraints

The constraints with inequality balance of the hybrid power model are the operational bounds of the generators, power system instruments and security of the power lines and the buses.

$$P_{TGi}^{min} \le P_{TGi} \le P_{TGi}^{max},\ i = 1, \cdots .., N_{TG} \tag{15}$$

$$P_{WGk}^{min} \le P_{WGk} \le P_{WGk}^{max}, k = 1, \cdots .., N_{WG} \tag{16}$$

$$P_{SPVl}^{min} \le P_{SPVl} \le P_{SPVl}^{max},\ l = 1, \cdots ., N_{SPV} \tag{17}$$

$$Q_{TGi}^{min} \le Q_{TGi} \le Q_{TGi}^{max},\ i = 1, \cdots ., N_{TG} \tag{18}$$

$$Q_{WGk}^{min} \le Q_{WGk} \le Q_{WGk}^{max},\ k = 1, \cdots ., N_{WG} \tag{19}$$

$$Q_{SPVl}^{min} \le Q_{SPVl} \le Q_{SPVl}^{max}, l = 1, \cdots , N_S \tag{20}$$

$$V_{Gi}^{min} \le V_{Gi} \le V_{Gi}^{max}, i = 1, \cdots ., NG \tag{21}$$

$$V_{L_p}^{min} \le V_{L_p} \le V_{L_p}^{max}, p = 1, \cdots , NL \tag{22}$$

$$S_{l_q} \le S_{l_q}^{max}, q = 1, \cdots ., nl \tag{23}$$

Here, N_{WG}, N_{WG} and N_{SPV} characterize the number of thermal generators, wind plants and solar photovoltaics correspondingly. The power production bounds of the thermal generators, wind generators and solar photovoltaic are represented in equations (15)–(17) respectively. Similarly, the equations (18)-(20) represent the limits of reactive power generators. Equations (21) and (22) represent the voltage constraints of the generator buses and load buses individually. The total quantity of bus generators, load buses and transmission lines are provided by NG, NL and nl respectively.

3. Objective functions and study cases

Eight cases studies are accomplished here to highlight the strength of the CSO algorithm in solving the 30-bus IEEE hybrid power system problem. The first 4 cases under goes the single objective functions of the HPS whereas the remaining 4 cases assess the multi-objective functions. The multi-objective functions are transformed into single objectives by adjusting suitable weight factors available in the literature. The considered case studies are listed as following.

3.1. Case No 1: Total cost minimization

The first case of the *HPS* combines all the cost functions of the power producing units by overlooking the consequence of the emission factor. Hence the first objective (F_1) is formulated to reduce the total cost as.

$$\begin{aligned} F_1 = Min\Big\{ & Fuel\ cost_{TG} + \sum_{k=1}^{N_{WG}} [Direct\ cost_{WGk}(P_{WGk}) \\ & + Reserve\ cost_{WGk}(P_{WGk} - P_{WGak}) \\ & + Penalty\ cost_{WGk}(P_{WGak} - P_{WGk})] + \sum_{l=1}^{N_{SPV}} [Direct\ cost_{SPVl}(P_{SPVl}) \\ & + Reserve\ cost_{SPVl}(P_{SPVl} - P_{SPVal}) + Penalty\ cost_{SPVl}(P_{SPVal} - P_{SPVl})]\Big\} \end{aligned} \tag{24}$$

3.2. Case No 2: Fuel cost minimization with effect of valve point

To model the hybrid power system in more realistic way, the effect of valve point is need to be reflected in the cost of the fuel. Hence, this case minimizes the fuel cost by considering the valve point effect as $F_2 = Min(F_1 + Valve\ Point\ Effect)$ (25).

3.3. Case No 3: Power loss minimization

For the existence of natural resistance in the lines, it becomes very difficult to avoid the transmission losses completely. Hence, case 3 considers to reduce the real loss of the power.

$$(MW)\ \text{as}\ F_3 = Min(Power\ loss) \tag{26}$$

3.4. Case No 4: Voltage deviation minimization

To maintain the voltage quality in hybrid power system it is very much necessary to regulate the voltage deviations. Therefore, the accumulative variation of the voltages of entire load buses is need to be reduced. Therefore, the objective for the case 4 is provided as follows.

$$F_4 = Min(Voltage\ deviation) \tag{27}$$

3.5. Case No 5: Total cost minimization with inclusion of emission cost

In recent times, several nations are placing immense burden on the whole energy area to lessen carbon emissions because of global warming. In order to promote the green energy resources as wind power, hydro power and solar power and carbon tax factor $(Carbon_{tax})$ is levied on each unit of poisonous gasses. Hence, the multi-objective scenario for the case is to reduce the total cost of the fuel along with the emission cost is provided as.

$$F_5 = Min(F_1 + Carbon_{tax} * Emission) \quad (28)$$

3.6. Case No 6: Power loss minimization and total cost minimization

In this case, the objectives power loss and total cost are transformed in to a solo objective by multiplying suitable weight factor ($\lambda_p = 40$)(Mohamed et al., 2017). Hence, the total objective for the case is to catch the best solution for both the objectives simultaneously as.

$$F_6 = Min(F_1 \times \lambda_p Power\ loss) \quad (29)$$

3.7. Case No 7: Voltage deviation and total cost minimization

The case 7 considers to reduce the cost of the fuel as well as the cumulative voltage abnormality concurrently. Hence, the objective function for the case is formed with help of suitable weight value ($\lambda_{VD} = 100$) (Bouchekara et al., 2016; Mohamed et al., 2017). The objective function is given as

$$F_7 = Min(F_1 + \lambda_{VD} \times Voltage\ deviation) \quad (30)$$

3.8. Case No 8: Total cost, carbon emission, voltage variation and power loss minimization

The last case combines all the four primary objectives simultaneously to assess the overall result. Hence, the objective function is formed by taking suitable weights ($\lambda_E, \lambda_{VD}$and λ_P)(Mohamed et al., 2017). The objective function for the last case is described as.

$$F_8 = Min(F_1 + \lambda_E \times Emission + \lambda_{VD} \times Voltage\ deviation + \lambda_P \times Power\ loss) \quad (31)$$

The objective of all the above mention case analysis are summarized in Table 4 for comparative analysis.

4. Optimization algorithm and implementation

The Competitive Swarm Optimizer (CSO) is a swarm inspired algorithm introduced by Cheng and Jin (Cheng and Jin, 2014) in 2015. The method is motivated from the coordinated behavior of ants, fishes, and birds. In recent times, the CSO algorithm has been recognized (Liang et al., 2006) as a metaheuristic algorithm in dealing challenging optimization problems easily. The CSO algorithm is basically motivated from the particle swarm optimization algorithm (PSO), but the operational technique of the CSO is much different from PSO and other evolutionary algorithms. The algorithm evades the situation of early convergence by entirely getting freed from global best position and personal best position. Hence, the CSO algorithm does not involve any memory to update the particles. Rather, the concept of competitive mechanism is introduced between the particles to get the work done. The first kind of such work was introduced by Liang (Liang and Suganthan, 2005) short of the global best position. Forth after, an identical idea was proposed in a multi-swarm design (LaTorre et al., 2015). Following to the idea, CSO exposed the exercise of pair wise competition between the members in one single swarm. In this scenario, the member that losses the competition motivates from the winner particle in place of personal best position and global best position. This notion of CSO algorithm is straight, however impressive enough to solve many optimization problems.

4.1. Motivation

In the CSO algorithm, the 50 % of the population is modernized in every iteration to move towards the winner particles for improving the convergence rate. The particles that win the competition are promoted to the next iteration to preserve the good solutions. This ensures the high diversity in the population. The inspiration behind the partition of the whole population into two populations is to maintain the balance between both the convergence speed and the diversity. The pair-wise competitive scenario of the CSO algorithm and the update process of loser particles are presented in Fig. 4.

Let the considered problem is $minFun(x)$where $x \epsilon X$ and $X \in R^m$ denotes the m-dimensional variable space and the primary swarm be U comprising r members at t^{th} iteration. Let the current position and current velocity of every member at t^{th} iteration are denoted by $x_i(t) = (x_{i,1}(t), x_{i,2}(t), \cdots, x_{i,m}(t))$ and $v_i(t) = (v_{i,1}(t), v_{i,2}(t), \cdots, v_{i,m}(t))$. In each iteration t, the members in population $P(t)$ are randomly distributed into two different populations. At that time, a pairwise competition is designed amid the members to choose the winner particles and loser particles. The particles that lose the competition (losers) improve their positions and velocities by inspiring from the particles that win the competition (winners). The position and velocity of the winner particles and loser particles in the k-th round of competition at iteration t are given as $x_{winner}(t), x_{losser}(t)$ and $v_{winner}(t), v_{losser}(t)$ respectively . After the k^{th}

Table 4
Case studies of the 30-bus IEEE HPS.

Cases	Total cost	Emission Cost	Power loss	Voltage deviation	effect of Valve point
Case No 1	✓				
Case No 2					✓
Case No 3			✓		
Case No 4				✓	
Case No 5	✓	✓			
Case No 6	✓		✓		
Case No 7	✓			✓	
Case No 8	✓	✓	✓	✓	

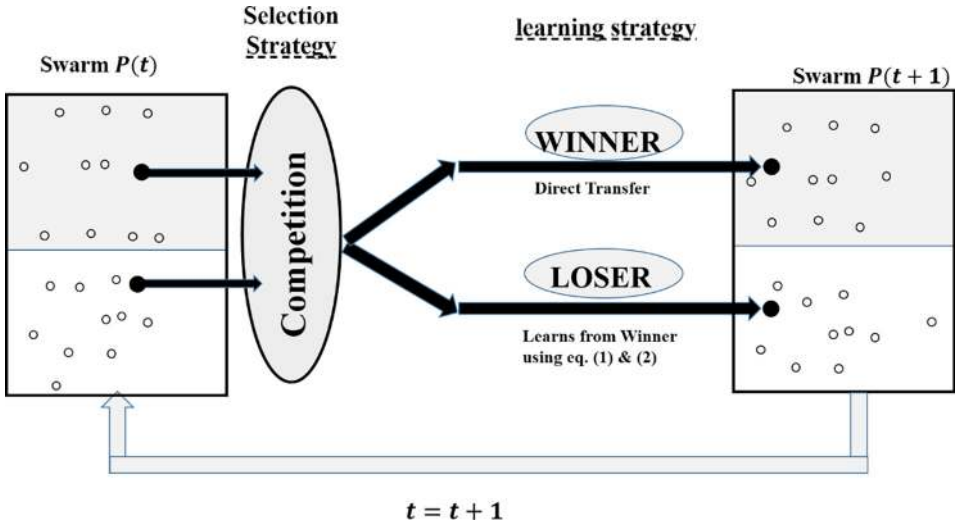

Fig. 4. The pair wise competitive mechanism in CSO and the upgrading approach.

time competition, the next iteration velocity and position of the losers are updated as.

$$v_{losser,k}(t+1) = R_1 v_{losser,k}(t) + R_2\left(x_{winner,k}(t) - x_{losser,k}(t)\right) + \varphi_1 R_3\left(\bar{x_k}(t) - x_{losser,k}(t)\right) \quad (32)$$

$$x_{losser,k}(t+1) = x_{losser,k}(t) + v_{losser,k}(t+1) \quad (33)$$

Here, R_1, R_2 and $R_3 \epsilon [0,1]^n$ are three arbitrarily produced vectors, $\bar{x_k}(t)$ is the mean position and φ_1 is the scalar factor. The pseudo-code of the CSO method is presented in the following algorithm. The flow chart for the adapted problem is provided in Fig. 5.

Algorithm: The pseudo code of the Competitive Swarm Optimization algorithm (CSO).

Here, the notation U means the initially generated swarm, $P(t)$ signifies the population elements at a specific iteration 't'. Similarly $X_{winner}(t)$ and $X_{losser}(t)$ denote the winner particles and loser particles. The *stopping criteria* is the overall function calculations.

1. Initialization
2. Arbitrarily generate the population $P(0)$;
3. **Do while** stopping criteria is not fulfilled
4. Calculate the objective function of the members in $P(t)$;
5. $U = P(t)$, $P(t+1) = \varnothing$;
6. **Do while** $U \neq \varnothing$
7. Choose two particles randomly $X(t)$ and $Y(t)$ from U;such that.$Fun(X(t)) \leq Fun(Y(t))$
1. Assign $X_{winner}(t) = X(t)\, and\, X_{losser}(t) = Y(t)$;
2. Add $X_{winner}(t)$ into $P(t+1)$;
3. Update $X_{losser}(t)$ to $X_{losser}(t+1)$ by eqn. (32–33) and add to $P(t+1)$;
4. Eliminate $X(t)$, $Y(t)$ from U;
5. **End**
6. $t = t + 1$;
7. **End**

5. Setup and analysis of the results

In this section, different case studies are carried out for the considered 30 bus IEEE hybrid power system problem. The eminent CSO along with other state-of-the-art algorithms such as GA, PSO, SHADE-SF, CSA, ABC, FPA and GPC are implemented to discover the outcomes for the case studies. In each case study, the size of the population (NP) is taken at 60 for all the methods. As a stopping criteria, the total function evaluations and total runs are fixed at 24,000 and 5 times respectively. The optimized results of the algorithms along with the 11 control variables and other parameter settings are tabulated and explained later in this section. These experiments are executed on a computer with Intel (R) Core (TM)$i57200UCPU@2.7GHz$ and $16GBRAM$ configuration. The direct cost coefficients (u_k)for the first wind power generator ($WG1$) and second wind power ($WG2$) generator are taken as 1.6 and 1.75 respectively. The penalty cost coefficients (K_{PWG1}, K_{PWG2}) and reserve cost coefficients (K_{RWG1}, K_{RWG2}) for the wind power generators are fixed at 1.5 and 3 correspondingly. Similarly the coefficients for direct cost (v_l), penalty cost (K_{PSPV1}) and reserve cost (K_{RSPV1}) for the solar power plant is fixed at 1.6, 1.5 and 3 respectively.

5.1. Cost effective scenarios

A number of cases studies are carried out to improve the performance of the hybrid power system on six generators IEEE 30-bus system consisting of three thermal power producing units, two windfarms and one solar photovoltaic plant. The effectiveness of the *HPS* is examined by considering three different configurations such as TS, TW and TWS. The first configuration TS is designed with thermal and solar power generating units. The second configuration TW is planned with thermal and wind power generating units. Similarly, the third configuration TWS is considered with thermal, wind and solar generating units. Further, the capability of each configuration is examined by introducing three different scenarios. Three scenarios operate with 10 %, 25 % and 35 % of the renewable energy respectively. The graphical representation of the configurations along with the scenarios is presented in Fig. 6.

The total cost of the hybrid power system configurations along with the scenarios are now optimized with the support of competitive swarm optimization method. The results are graphically picturized in Fig. 7. From this graph, it is clearly perceived that with the increase uses of renewable energy, the operating cost of TWS configuration is far superior to TS and TW models. The reason for the type of behavior of the hybrid power system is due to the substantial dependency on other non-renewable energy power generating units when the percentage of the renewable energy is low. The savings in operating cost of the TWS configuration with

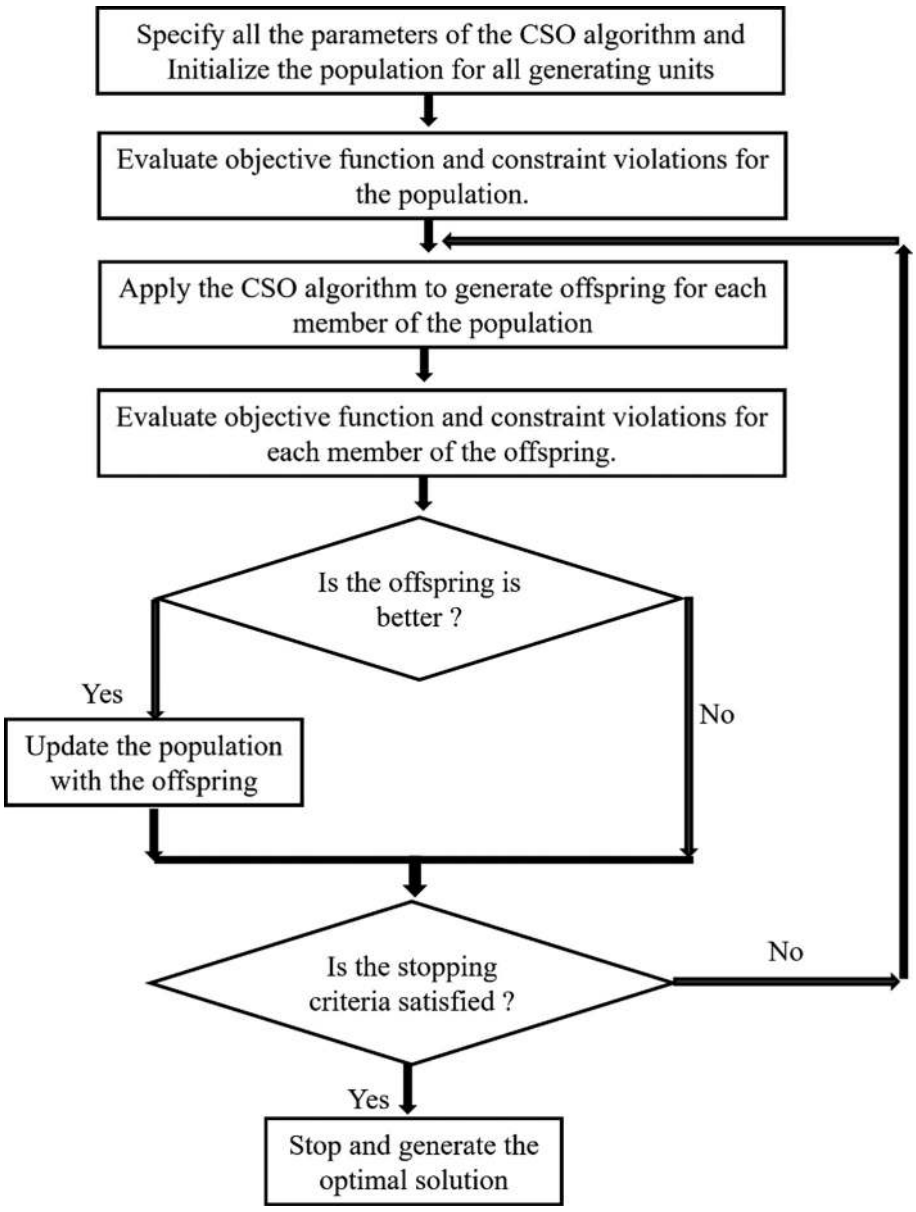

Fig. 5. Flowchart of the CSO technique in handling the HPS problem.

respect to TS and TW configuration is recorded in Table 5. In this table, it can be concluded that the selection of TWS configuration over TS and TW can result superior savings in terms of operating cost. Therefore, the TWS configuration is adapted in this paper to carry out all the following investigations of the considered problem.

5.2. Experimental results and comparison

In this part, first of all the state-of-the-art algorithms such as CSO, SHADE-SF, CSA, ABC, FPA and GPC are applied to find the best optimum values for all the eight cases acknowledged in section 3. The best fitness values along with their control variables and the parameters for the case 1 and case 5 are provided in Tables 6a and 6b respectively. The overall results of each case study is reflected in Table 7. From the Tables, it is witnessed that the fuel cost of Case 1 is 781.889 $/h$ for CSO is the best among all the state-of-the-art algorithms. The CSO algorithm is able to provide optimum fuel cost value than the other algorithms by balancing all the constraints. It is also realized that, the violations for the constraints are adjusted crucially to achieve the result and all the parameters and the control variables and are also balanced in their permitted limits. Effect of valve point is undertaken in case 2 to notice an increased cost for the algorithms. However the supremacy of CSO algorithm is remain unchanged. The case 3 considers the performance of the algorithms in term of real power losses. As the power loss is an important factor for optimum power flow problem, hence the performance of the CSO algorithm cannot be disregarded with respect to the other algorithms. The real power loss for the algorithm CSO is 2.0751 *MW*. The voltage deviation parameter examined in case 4 accomplishes very closed result with SHADE-SF algorithm.

The remaining four cases are the multi-objective scenarios. The case 5 represents the reduction of fuel cost with the inclusion of emission cost. The current observation with CSO finds an enhanced and better cost 810.31982$/h$ than the cost of the SHADE-SF and other algorithms. The CSO algorithm tries to provide the optimum solution for both the objectives. Case 6 and case 7 consider fuel

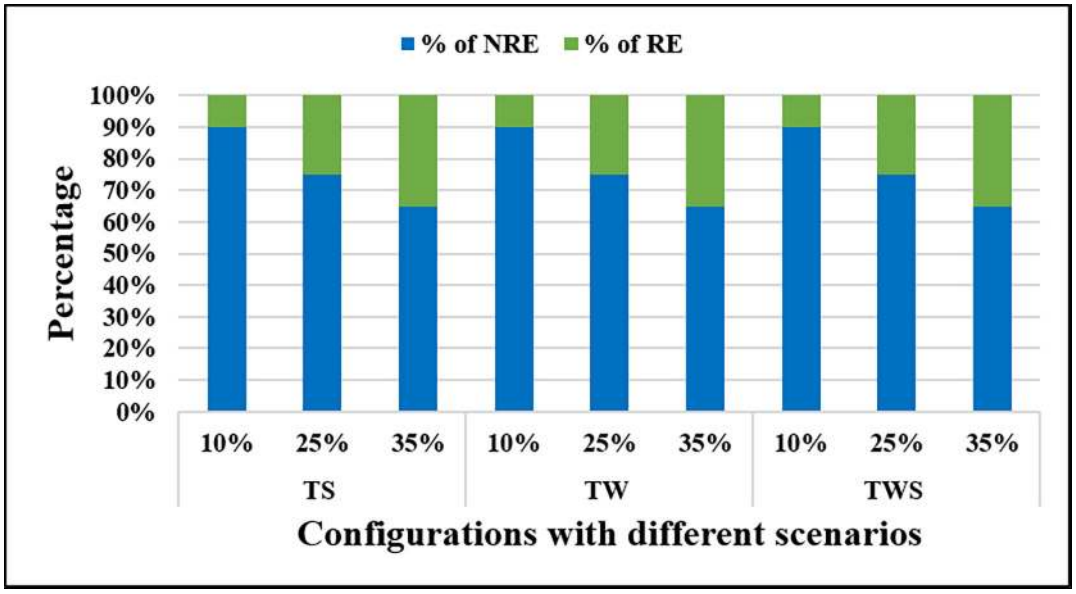

Fig. 6. Hybrid power system configurations with different scenarios.

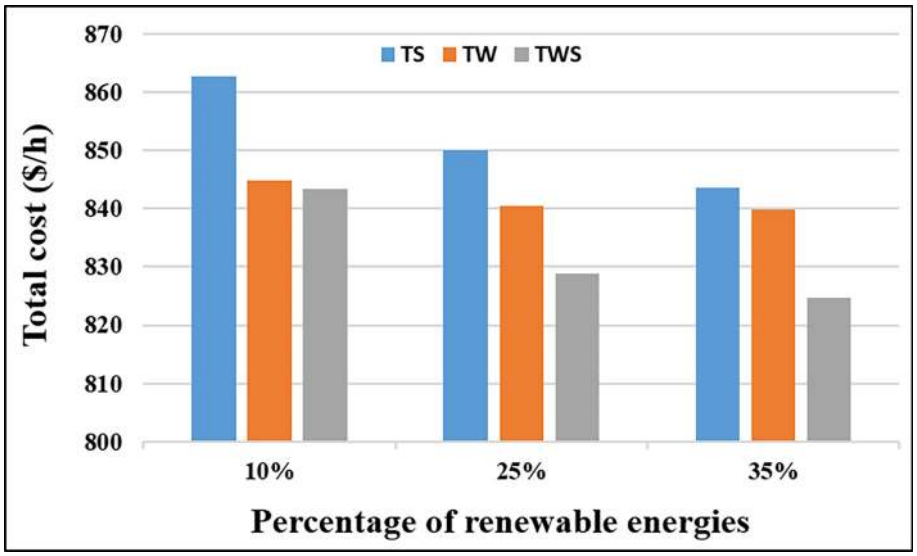

Fig. 7. Total cost of different hybrid power system configurations at different scenarios.

Table 5
Savings in operating cost of TWS with respect to TS and TW respectively.

	Renewable percentages	TWS compare to TS	TWS compare to TW
Savings in operating cost ($/h$)	10 %	19.3846	1.5389
	25 %	21.2627	11.777
	35 %	18.8079	15.2453
Savings in operating cost ($/year$)	10 %	169809.09	13480.76
	25 %	186261.25	103166.52
	35 %	16477.20	133548.82

cost along with power loss and voltage deviation respectively, whereas case 8 considers all the four primary objectives fuel cost, power loss, emission and voltage deviation simultaneously. In all these multi-objective cases, the effectiveness of the CSO algorithm is much better to the SHADE-SF and other algorithms. It can be clearly observed from the above analysis that the results of CSO algorithm is promising and encouraging in 7 cases out of 8 considered cases when compared with the near competitor SHADE-SH algorithm. The convergence graphs of the cases are also drawn in Fig. 8 to justify the claim. The convergence graphs of the Fig. 8 also confirm the superiority of the CSO algorithm in all the 7 cases. Further, some statistical analyses are also performed in next section to investigate the significant difference between the algorithms.

5.3. Statistical test

In this part, three types of statistical measures are considered to analyze the results which are mention as follows.

5.3.1. Mean, standard deviation and *t*-test

Let $x_1, x_2, \cdots\cdots\cdots x_N$ be the attained solutions of the N independent runs. Then the best result, worst result, mean(μ) and std(σ) for all the case studies are listed in Table 7. The mean (μ) and

Table 6a
Best computational results of the HPS for the case 1.

Control variables	Min	Max	Case 1							
Algorithms			SHADE-SF	CSO	GA	PSO	CSA	ABC	FPA	GPC
*PTG*1(*MW*)	50	140	134.9079	134.9114	134.90	134.90	134.90	134.80	134.90	134.92
*PTG*2(*MW*)	20	80	29.1983	28.4860	32.10	31.40	30.50	28.60	28.22	29.32
*PTG*3(*MW*)	10	35	10.0000	10.0063	15.20	10.00	10.00	10.00	10.00	10.00
*PWG*1(*MW*)	0	75	44.1585	43.7873	41.80	43.80	44.50	44.40	42.34	43.39
*PWG*2(*MW*)	0	60	37.2400	36.8945	33.70	37.40	37.80	39.00	36.51	37.61
*PSPV*1(*MW*)	0	50	33.7550	35.0902	31.80	32.50	31.90	32.40	37.29	33.97
*V*1(*p.u.*)	0.95	1.10	1.0738	1.0718	1.02	1.050	1.040	1.060	1.069	1.068
*V*2(*p.u.*)	0.95	1.10	1.0145	1.0567	1.01	0.950	0.900	1.030	1.056	1.050
*V*5(*p.u.*)	0.95	1.10	1.0382	1.0339	1.02	1.000	0.900	1.010	1.027	1.036
*V*8(*p.u.*)	0.95	1.10	1.0995	1.0590	1.00	1.030	1.000	1.040	1.074	1.096
*V*11(*p.u.*)	0.95	1.10	1.0999	1.0970	1.03	0.950	1.010	1.090	1.088	1.098
*V*13(*p.u.*)	0.95	1.10	1.0631	1.0498	1.05	1.010	1.040	1.01	1.061	1.100
*QTG*1(*MVAr*)	−20	150	16.79819	−2.00046	−1.64	48.80	31.40	30.880	−5.548	2.768
*QTG*2(*MVAr*)	−20	60	−20.00000	12.17394	6.57	−20.00	−20.00	−15.50	19.594	−6.701
*QTG*3(*MVAr*)	−15	40	40.0000	40.00000	40.00	40.00	40.000	36.645	40.000	40.000
*QWG*1(*MVAr*)	−30	35	30.13183	21.66628	35.00	35.00	30.030	23.794	16.207	27.391
*QWG*2(*MVAr*)	−25	30	30.0000	29.63473	21.00	−3.40	15.600	29.636	26.420	28.966
*QSPV*1(*MVAr*)	−20	25	20.45997	15.50949	20.00	22.70	25.00	10.40	20.480	25.000
Fuel cost (/*h*)			782.86750	**781.88998**	787.84	785.82	784.770	782.859	782.859	782.422
Emission (*ton*/*h*)			1.76192	1.76140	2.760	2.360	1.960	1.762	1.762	1.764
P_{loss} (*MW*)			5.897	5.7713	6.430	6.790	6.470	5.863	5.863	5.843
VD (*p.u.*)			0.49450	0.45234	0.870	1.080	0.850	0.455	0.455	0.537

Table 6b
Best computational results of the HPS for the case 5.

Control variables	Min	Max	Case 5							
Algorithms			SHADE-SF	CSO	GA	PSO	CSA	ABC	FPA	GPC
*PTG*1(*MW*)	50	140	123.525	123.7114	122.90	123.20	122.80	123.60	124.13	124.00
*PTG*2(*MW*)	20	80	33.047	33.5415	35.60	33.80	31.40	34.40	34.22	34.00
*PTG*3(*MW*)	10	35	10.0000	10.0029	14.40	10.00	10.00	10.00	10.01	10.00
*PWS*1(*MW*)	0	75	46.021	46.3004	45.30	45.30	45.50	46.80	46.66	46.39
*PWS*2(*MW*)	0	60	38.748	38.9339	36.90	36.90	38.30	37.30	38.57	39.04
*PSPV*1(*MW*)	0	50	37.336	36.1895	33.70	39.40	40.60	36.30	35.09	35.27
*V*1(*p.u.*)	0.95	1.10	1.071	1.0701	1.030	1.100	1.070	1.070	1.070	1.069
*V*2(*p.u.*)	0.95	1.10	1.057	1.0564	1.020	1.030	1.060	1.060	1.055	1.054
*V*5(*p.u.*)	0.95	1.10	1.036	1.0353	1.000	1.090	1.060	1.080	1.038	1.030
*V*8(*p.u.*)	0.95	1.10	1.04	1.0424	1.020	1.070	1.040	1.040	1.052	1.099
*V*11(*p.u.*)	0.95	1.10	1.099	1.0985	1.040	1.040	1.000	1.090	1.095	1.086
*V*13(*p.u.*)	0.95	1.10	1.056	1.0534	1.020	1.040	1.050	1.050	1.053	1.099
*QTG*1(*MVAr*)	−20	150	−2.678	−2.65848	−1.760	36.500	−1.560	−3.000	−0.379	−0.139
*QTG*2(*MVAr*)	−20	60	12.319	10.44618	9.930	−20.00	20.830	12.840	4.145	6.648
*QTG*23(*MVAr*)	−15	40	35.27	39.05657	40.00	40.00	40.00	27.430	40.00	40.00
*QWG*1(*MVAr*)	−30	35	22.964	22.10929	28.660	35.00	35.00	35.00	25.942	19.021
*QWG*2(*MVAr*)	−25	30	30	30.00000	21.280	9.880	−0.490	27.480	28.844	25.052
*QSPV*1(*MVAr*)	−20	25	17.779	16.71581	20.450	12.750	21.550	15.190	17.018	25.00
Total cost (/*h*)			810.346	**810.31982**	814.720	811.490	811.530	811.260	811.666	810.324
Emission (*ton*/*h*)			0.891	0.88467	1.360	0.980	0.920	0.890	0.923	0.916
P_{loss} (*MW*)			5.276	5.2844	5.630	5.460	5.440	5.310	5.307	5.327
VD (*p.u*)			0.469	0.46542	0.640	0.480	0.490	0.470	0.465	0.507

Table 7
Overall statistical summary of considered case studies for the HPS problem.

Cases	CSO				SHADE-SF				*t*-value
	Best	Worst	Mean	Std	Best	Worst	Mean	Std	
Case 1	**781.889**	782.193	782.020	0.14796	782.867	783.886	783.472	0.43394	**−7.07E + 00**
Case 2	**249.243**	249.243	249.242	0.00044	249.245	249.245	249.250	0.00000	**−5.08E + 01**
Case 3	**2.07542**	2.10603	2.07910	0.00721	2.1037	2.10371	2.10371	0.01621	**−3.10E + 00**
Case 4	0.37576	0.37578	0.37580	0.00001	**0.37523**	0.37576	0.37540	0.00029	3.08E + 00
Case 5	**810.319**	811.082	810.622	0.21356	810.346	811.694	811.180	0.46617	**−2.44E + 00**
Case 6	**958.700**	958.849	958.762	0.06739	958.790	959.552	959.090	0.26696	**−2.68E + 00**
Case 7	**824.418**	824.685	824.480	0.11664	824.673	825.598	825.350	0.38689	**−4.81E + 00**
Case 8	**922.617**	922.716	922.670	0.16818	922.953	923.804	923.360	0.38979	**−3.63E + 00**
w/*t*/*l*									7/0/1

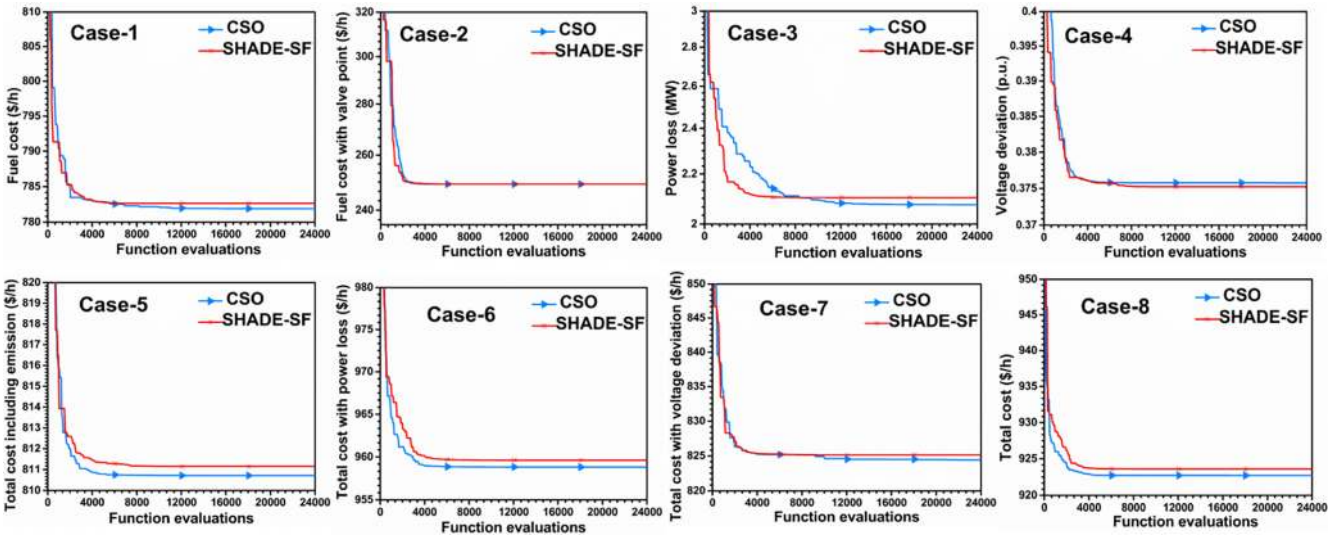

Fig. 8. Convergence graph between SHADE-SF and CSO algorithm.

the std(σ) of N independent runs are calculated by the following equations (34) and (35) respectively.

$$\text{Mean } (\mu) = \frac{\sum_{i=1}^{N} x_i}{N} \tag{34}$$

$$\text{Standard deviation } (\sigma) = \frac{\sqrt{\sum_{i=1}^{N} (x_i - \mu)^2}}{N} \tag{35}$$

Due to the small sample size ($N < 30$), the statistical *t-test* with 5 % of LOS is adopted to observe the statistical gap between the means of the algorithms. Let the means and standard deviations of the algorithms CSO and its competitor are given by μ_1, μ_2 and σ_1,σ_2 individually. Then the t-values are generated by using the equation (36) and the values are listed in Table 7. From the t-test formula it is clear that, a negative t-value represents superior solution of the CSO algorithm than it's near competitor SHADE-SF algorithm. Similarly a positive t-value represents superior solution of SHADE-SF algorithm than the CSO algorithm. Hence, the negative t-values are considered as the wins and positive t-values are considered as losses. If the solutions are statistically insignificant to each other then, the corresponding t-value is considered as a tie. The t-values of the wins are boldfaced whereas the t-values of the ties are highlighted with italic. The heading $w/t/l$ totals the number of win cases, tie cases and loss cases respectively.

$$t\text{-test } (t) = \frac{\mu_1 - \mu_2}{\sqrt{\frac{{\sigma_1}^2 + {\sigma_2}^2}{N}}} \tag{36}$$

Table 8
Average ranking and comparison of best count between CSO and SHADE-SF.

	SHADE-SF		CSO	
Cases	Average Ranking	Best Count	Average Ranking	Best Count
Case No 1	2.00	0	**1.00**	**4**
Case No 2	1.75	1	1.25	3
Case No 3	1.75	1	1.25	3
Case No 4	1.75	1	1.25	3
Case No 5	1.75	1	1.25	3
Case No 6	1.5	2	1.5	2
Case No 7	1.25	3	1.75	1
Case No 8	1.75	1	1.25	3

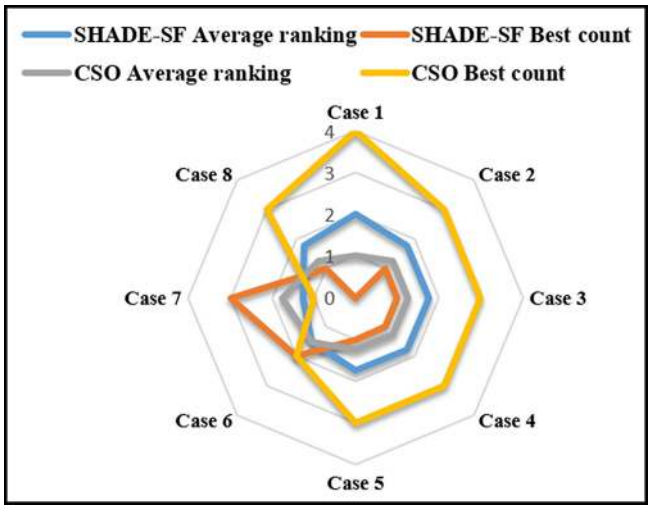

Fig. 9. Radar chart for the average ranking and best count for CSO and SHADE-SF.

From the results of Table 7, the dominance behavior of the CSO algorithm is witnessed at 7 cases in terms of best solutions. In the remaining one case (Case 4) the SHADE-SF algorithm is capable to achieve superiorly than the CSO algorithm. Similar analysis can also be drawn from the $w/t/l$ heading. For the CSO algorithm the number of wins (w) is 7, whereas the number of losses (l) is 1 in comparison to the SHADE-SF algorithm. There exists no case where the solutions of both the algorithms are insignificant to each other. This means that the number of ties (t) is zero.

5.3.2. Friedman's average ranking test and best count test

In this section, the Friedman ranking test (Mishra et al., 2020) is applied to find the significance difference between the methods in terms of multiple comparisons by considering all the fitness values. The relative ranking of the algorithms are first computed according to their performances in each objective function. Then the average ranking is calculated by taking the mean of the relative rankings. The average ranking of the algorithms for the four primary objectives like total cost, carbon emission, voltage variation and power loss in each case is computed and listed in Table 8. The best count of a method is defined as the number of objective functions for

Table 9
Simulation results by variation in reserve cost coefficient for hybrid power system.

KP = 1.5 (Fixed)	KR = 3		KR = 4		KR = 5		KR = 6	
	SHADE-SF	CSO	SHADE-SF	CSO	SHADE-SF	CSO	SHADE-SF	CSO
*TG*1(*MW*)	134.90	134.91149	134.90791	134.93261	137.65158	137.33158	140.00000	139.96904
*TG*2(*MW*)	28.564	28.4860	41.8381	42.6195	53.7258	53.6453	58.2046	57.6622
*TG*3(*MW*)	10	10.0063	10.0000	10.0380	10.0000	10.0693	13.9788	14.0775
*WG*1(*MW*)	43.774	43.7873	37.6301	37.8827	32.4680	32.4660	27.8321	27.9728
*WG*2(*MW*)	36.949	36.8945	32.3415	32.5717	28.2840	28.2617	24.4704	24.4741
SPV(*MW*)	34.976	35.0902	33.0105	31.5857	28.0642	28.4013	26.0504	26.3609
TOTAL COST ()	782.503	781.88998	821.2068	821.1503	851.2262	850.9534	873.9042	873.5189
TG COST ()	439.8337	442.06528	487.0547	490.1335	541.3847	540.171	583.1	581.2898
WG COST ()	245.5489	248.0038	236.8486	238.6757	223.9132	223.8175	207.6672	208.2573
SPV COST ()	97.1204	91.8209	97.3035	92.3411	85.9283	86.9649	83.1370	83.9718
Fuel valve cost ()	439.9944	442.0653	487.0547	490.1336	541.3847	540.1710	583.1000	581.2899
Emission (*ton*/*h*)	1.762	1.76140	1.76003	1.76266	2.08700	2.04574	2.41758	2.41277
Real power loss (*MW*)	5.770	5.7713	6.3281	6.2301	6.7936	6.7752	7.1363	7.1165
Cumulative voltage drop (*p.u*)	0.463	0.45234	0.48247	0.47787	0.44758	0.44518	0.44496	0.44564

Table 10
Simulation results by variation in penalty cost coefficient for hybrid power system.

KR = 3 (Fixed)	KP = 1.5		KP = 3		KP = 4		KP = 5	
	SHADE-SF	CSO	SHADE-SF	CSO	SHADE-SF	CSO	SHADE-SF	CSO
TG1 (MW)	134.908	134.91149	134.90791	134.90784	134.90791	134.90360	134.90791	134.90790
TG2 (MW)	28.564	28.4860	20.0268	20.8696	20.0000	20.0008	20.0000	20.0049
TG3 (MW)	10	10.0063	10.0000	10.0098	10.0000	10.0029	10.0000	10.0020
WG1 (MW)	43.774	43.7873	45.1367	45.5900	47.0160	46.2159	45.2016	44.9044
WG2 (MW)	36.949	36.8945	38.9197	39.1164	40.8594	40.4433	39.6722	39.0367
SPV (MW)	34.976	35.0902	40.0219	38.5075	36.1350	37.3851	39.2107	40.1637
TOTAL COST ($)	782.503	781.88998	800.4754	800.2546	810.9795	810.8348	822.8737	822.2662
TG COST($)	439.8337	442.06528	413.4823	416.1114	413.4003	413.4039	413.4004	413.4233
WG COST($)	245.5489	248.0038	268.2662	270.3379	286.5469	282.8348	284.1433	281.6550
SPV COST($)	97.1204	91.8209	118.7269	113.8053	111.0323	114.5961	125.3300	127.1879
Fuel valve cost($)	439.9944	442.0653	413.4822	416.1114	413.4004	413.4040	413.4004	413.4233
Emission (ton/h)	1.762	1.76140	1.76457	1.76427	1.76458	1.76411	1.76458	1.76458
Real power loss (MW)	5.770	5.7713	5.6129	5.6012	5.5183	5.5516	5.5925	5.6196
Cumulative voltage drop (p.u)	0.463	0.45234	0.45733	0.46299	0.45557	0.45819	0.46558	0.46111

which the method delivers the best solution in comparison to other methods. Here also the four primary objectives are considered. The best count for both the algorithms is noted down subsequently to the average ranking in Table 8. From these results, it can be observed that the average ranking and the best count for the CSO algorithm are superior to the SHADE-SF algorithm in most of the cases. It can also be pointed out that although the case 1 is designed to optimize the total cost, but the CSO algorithm is capable to provide the best solution for all the objectives. This results the best average ranking and maximum best count values. To describe the difference graphically, the average ranking and the best count values are picturized in Fig. 9 with the help of radar chart.

5.4. Case studies of variations in reserve and penalty coefficients

This section investigates the effects of reserve cost and penalty cost coefficients on the four primary objectives of the considered problem. At first reserve cost coefficients ($K_{RWG1} = K_{RWG2} = K_{RSPV1} = KR$) for the both wind and solar power system are changed from 3 to 6 with difference of 1 unit whereas, the penalty cost coefficients ($K_{PWG1} = K_{PWG2} = K_{PSPV1} = KP$) are remain unchanged. In second case, the penalty cost coefficients are varied from 1.5 to 3, 4 and 5 whereas the reserve cost coefficients are remain unchanged. The penalty cost and reserve cost coefficients affect the energy output at the generators. With the increase in reserve cost coefficients, the production at wind and solar power generators decreases. This results in enhanced production at thermal power generators. Hence it fuels the total cost. Similarly, the demand at thermal power generators decreases with increase of penalty cost coefficients. The increased penalty cost coefficient catalyzes the production of renewable energies. The Tables 9 and 10 list the results with the variations of the reserve cost and penalty cost coefficients correspondingly. The generated power from six plants with the variations of reserve cost and penalty cost coefficients for both the algorithms are graphically presented in Fig. 10(a-f) and Fig. 12(a-f) respectively. Similarly, the change of four types of costs with variations of the reserve cost and penalty cost coefficients are picturized in Fig. 11 and Fig. 13 respectively. From these tables and figures, the contradictory characteristics between the reserve cost coefficients and penalty cost coefficients are clearly established. The reserve cost coefficients in Table 9 represent the sharp increase of the thermal power cost as well as the emission values which results in drop of renewable energy power cost. But the penalty cost coefficients in Table 10 represent the firm decrease of the thermal power cost and surge in cost of renewable energies.

5.5. Variations in voltage deviation

In hybrid power system problem, the constraints on load buses voltage are very crucial in maintaining the voltage quality and security. Often the operating voltages tend to fall near their boundary limits. In the adopted problem, the load bus voltages are needed to be retained in between 0.95 and *p.u*.1.05 *p.u*. in order to achieve both the objectives. The voltage parameter for each

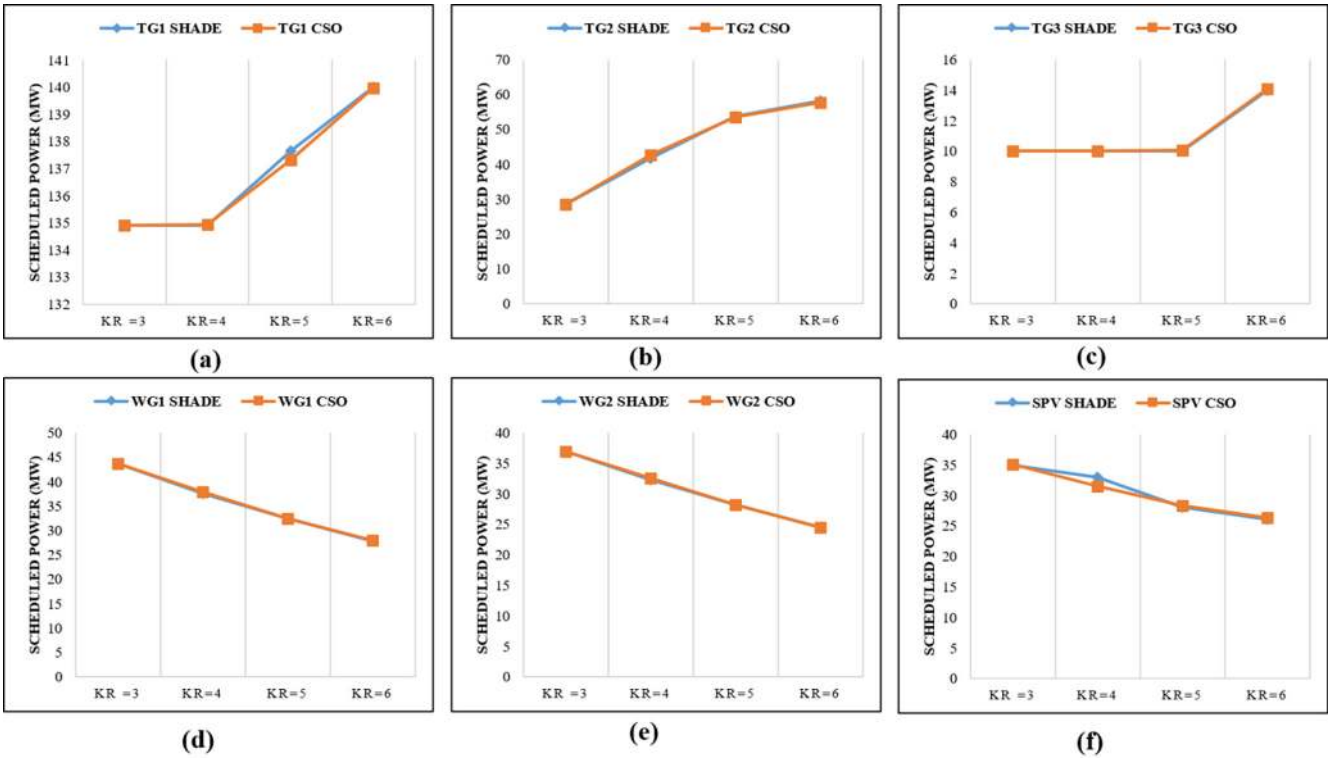

Fig. 10. Optimum generated power (*MW*) vs reserve cost coefficient for CSO and SHADE-SF.

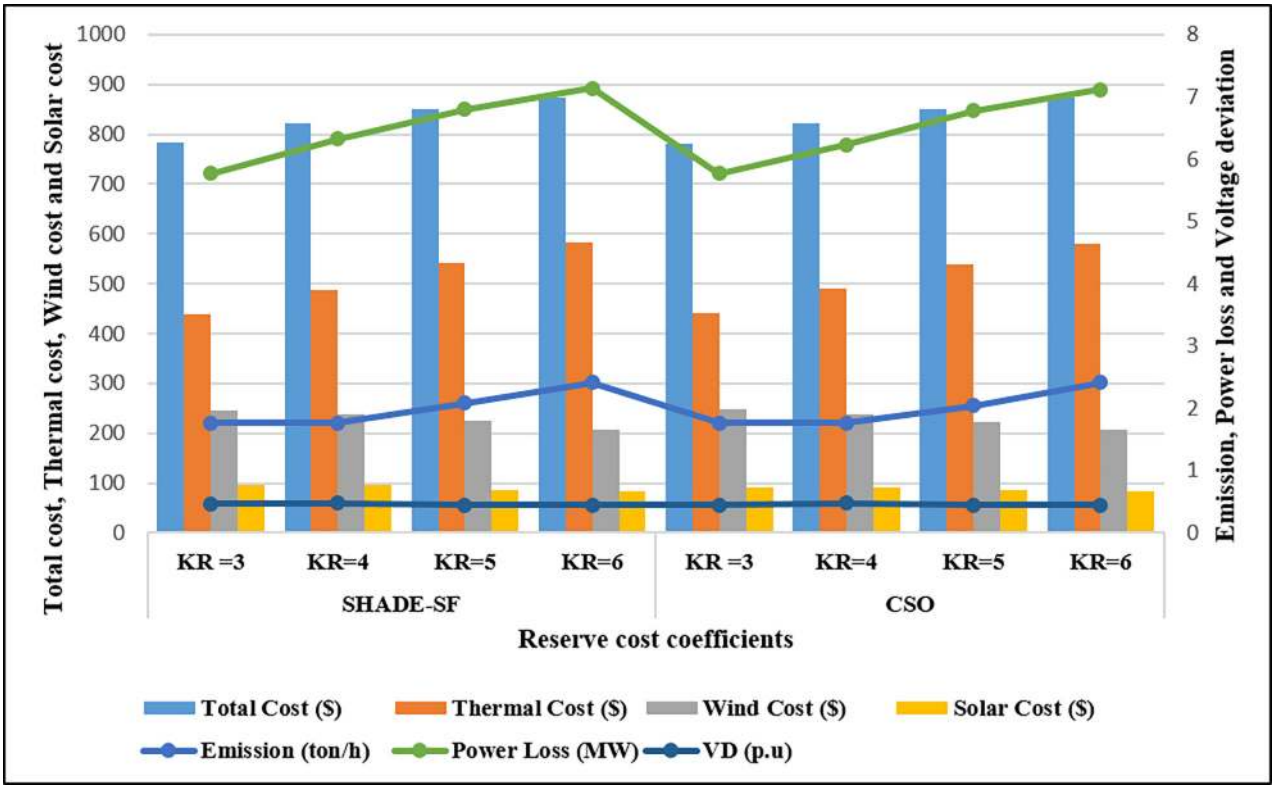

Fig. 11. Comparison of optimum output for variation in reserve cost coefficient between CSO and SHADE-SF.

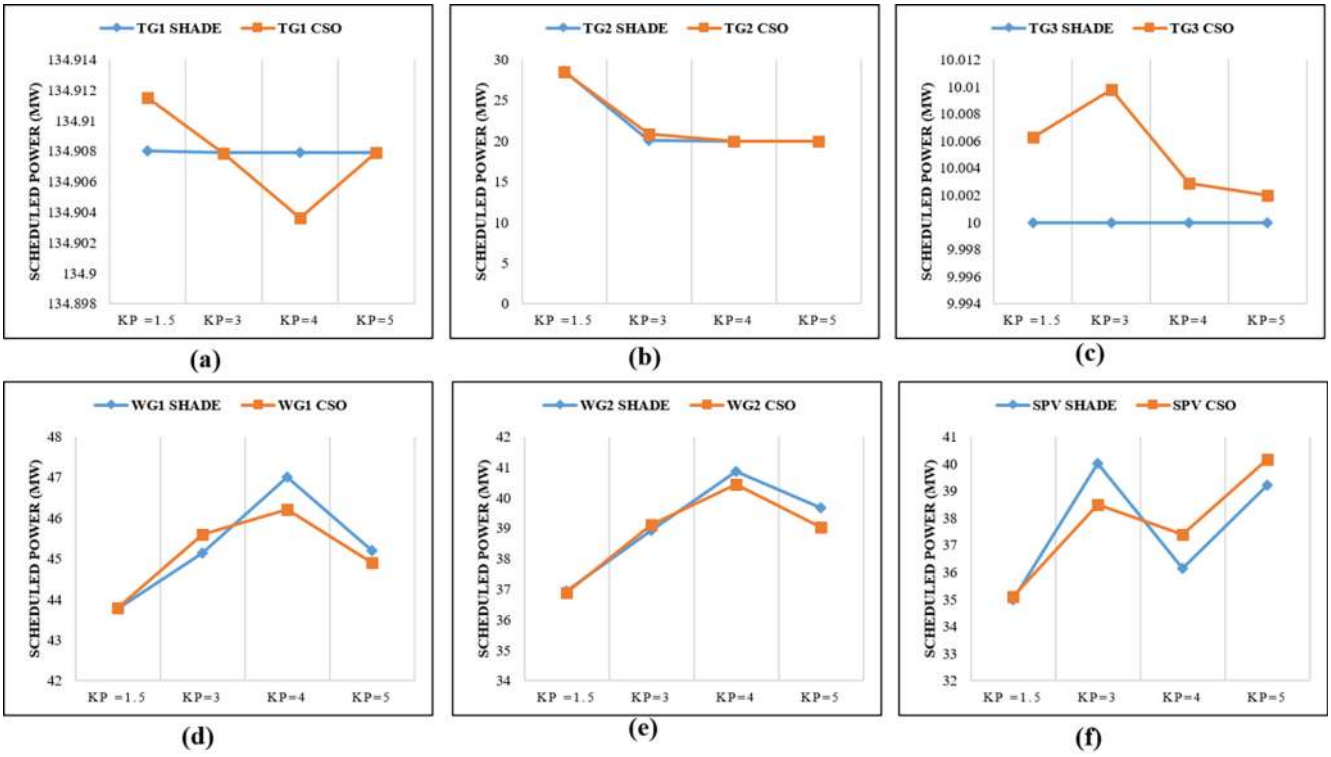

Fig. 12. Optimum generated power (*MW*) vs penalty cost coefficient for CSO and SHADE-SF.

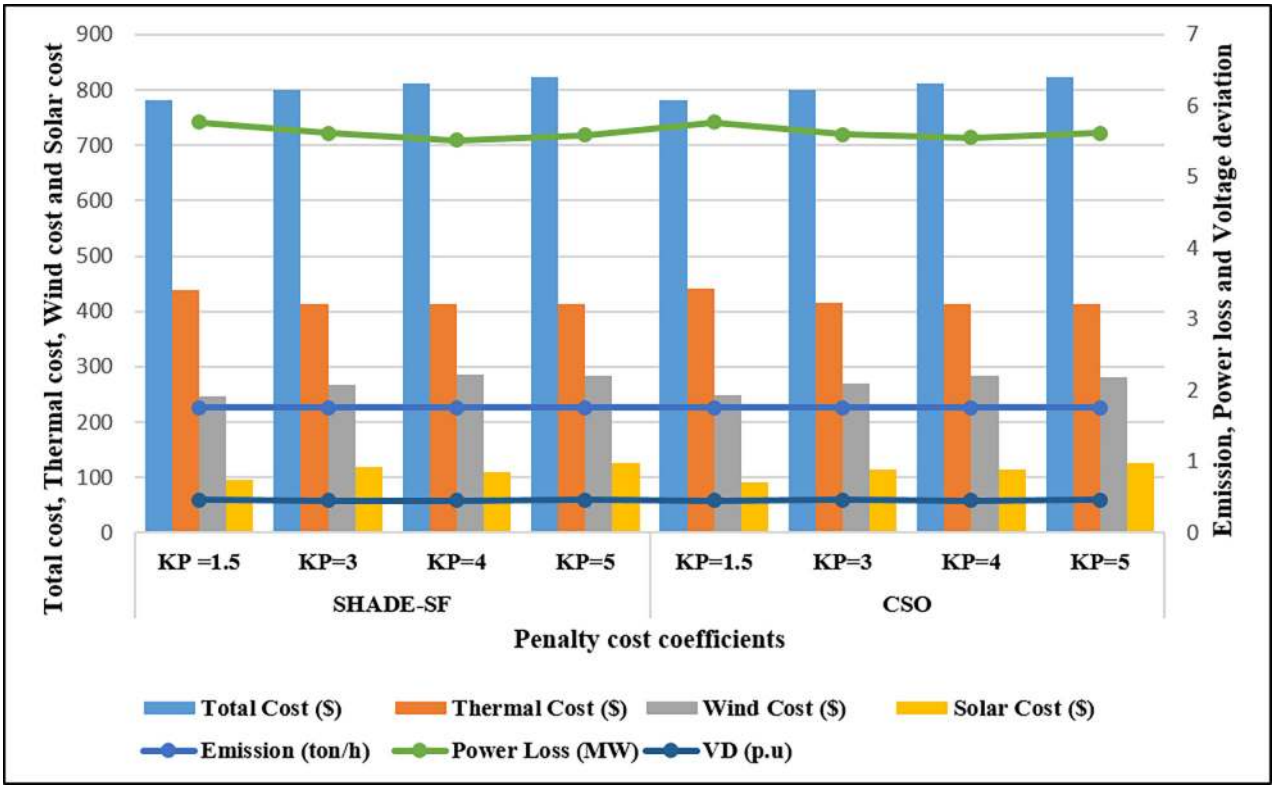

Fig. 13. Comparison of optimum output for variation in penalty cost coefficient between CSO and SHADE-SF.

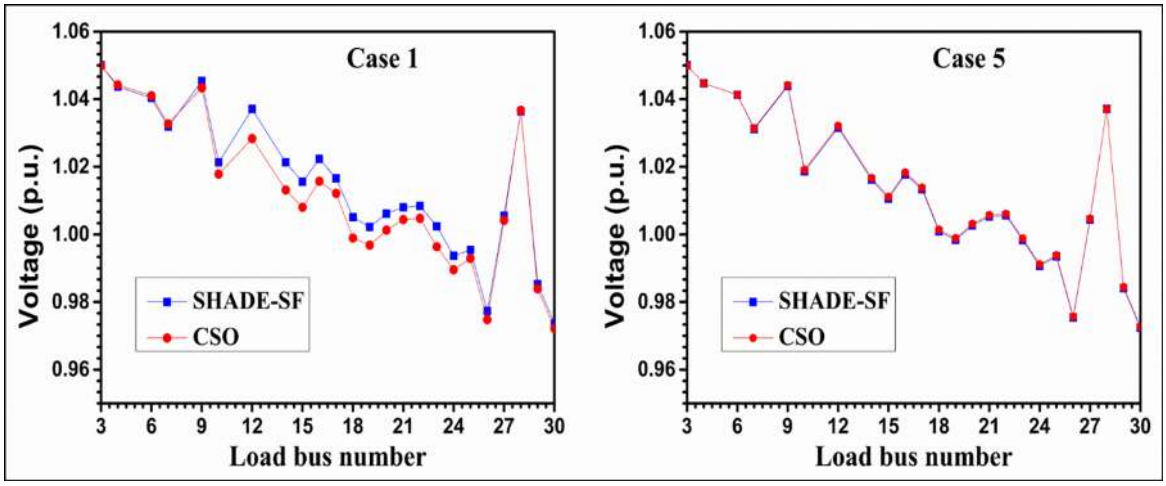

Fig. 14. Load bus voltage distribution for case 1 and case 5.

bus for the case No 1 and case No 5 are drawn in Fig. 14 to notice the variations. From the figure, it is clearly found that the voltage at individual bus is falling within the recommended boundaries. Similarly the load bus voltage analyses for other remaining cases are also found to follow identical patterns.

6. Conclusion

In this paper, an IEEE 30-bus hybrid power system (HPS) consisting of thermal and renewable energies is considered to minimize the emission of greenhouse gases and generation cost. The uncertain circumstances such as underestimation and overestimation are addressed with penalty cost and reserve cost respectively. A cost effective analysis also has been incorporated by proposing three hybrid configurations such as TS, TW and TWS. This analysis justifies the TWS configuration for substantial remunerations in terms of minimizing operating cost. Several state-of-the-art *meta*-heuristics are also implemented to provide the optimum scheduling among the generators by considering several case studies of single and multi-objectives. The experimental outcomes claim that the CSO algorithm not only delivers improved robust solutions but also it may be successfully applied in large scaled, non-convex and nonlinear hybrid power system optimization problems due to its better solution quality and fast convergence. However, the difficult hybrid power system problem of 57 and 117 buses are yet to be considered in the present work. This can be treated as the limitations, nevertheless it may also be treated as a future scope of the current work which needs to be addressed later.

Declaration of Competing Interest

The authors declare the following financial interests/personal relationships which may be considered as potential competing interests: I acknowledge VIT for providing VIT SEED GRANT for carrying out this research work.

References

I.E.A., 2019. Key World Energy Statistics. 6, 36.
Destek, M.A., Sinha, A., 2020. Renewable, non-renewable energy consumption, economic growth, trade openness and ecological footprint: evidence from organization for economic Co-operation and development countries. J. Cleaner Prod. 242, 1–11.
Li, L.L., Liu, Y.W., Tseng, M.L., Lin, G.Q., Ali, M.H., 2020. Reducing environmental pollution and fuel consumption using optimization algorithm to develop combined cooling heating and power system operation strategies. J. Cleaner Prod. 247, 119082.
Li, L.L., Zhao, X., Tseng, M.L., Tan, R.R., 2020. Short-term wind power forecasting based on support vector machine with improved dragonfly algorithm. J. Cleaner Prod. 242, 1–12.
Mahor, A., Prasad, V., Rangnekar, S., 2009. Economic dispatch using particle swarm optimization: a review. Renew. Sustain. Energy Rev. 13, 2134–2141.
Chaib, A.E., Bouchekara, H., Mehasni, R., Abido, M.A., 2016. Optimal power flow with emission and non-smooth cost functions using backtracking search optimization algorithm. Int. J. Electr. Power Energy Syst. 81, 64–77.
Bouchekara, H., Chaib, A.E., Abido, M.A., El-Sehiemy, R.A., 2016. Optimal power flow using an improved colliding bodies optimization algorithm. Appl. Soft Comput. 42, 119–131.
Mohamed, A.A.A., Mohamed, Y.S., El-Gaafary, A.A., Hemeida, A.M., 2017. Optimal power flow using moth swarm algorithm. Electric Power Syst. Res. 142, 190–206.
H.R., 1990. Congressional Amendment to the Constitution. 1490.
Lu, C., Tong, Q., Liu, X., 2010. The impacts of carbon tax and complementary policies on Chinese economy. Energy Policy 38 (11), 7278–7285.
Panda, A., Mishra, U., Tseng, M.-L., Ali, M., 2020. Hybrid power systems with emission minimization: multi-objective optimal operation. J. Cleaner Prod. https://doi.org/10.1016/j.jclepro.2020.121418.
Hetzer, J., Yu, D.C., Bhattarai, K., 2008. An economic dispatch model incorporating wind power. IEEE Trans. Energy Convers. 23, 603–611.
Jabr, R.A., Pal, B.C., 2009. Intermittent wind generation in optimal power flow dispatching. IET Gener. Transm. Distrib. 3 (1), 66–74.
Liu, X., Xu, W., 2010. Minimum emission dispatch constrained by stochastic wind power availability and cost. IEEE Trans. Power Syst. 25, 1705–1713.
Liu, X., 2011. Emission minimization dispatch constrained by cost and wind power. IET Generat. Transmission Distrib. 5, 735–742.
Wei, Z., Yu, P., Hui, S., 2011. Optimal wind–thermal coordination dispatch based on risk reserve constraints. Eur. Transact Elect Power 21 (1), 740–756.
Henerica, T., Bing, Z., Xiaohua, X., 2015. Optimal power flow management for distributed energy resources with batteries. Energy Convers. Manage. 102, 104–110.
Kanzumba, K., 2016. Optimal scheduling for distributed hybrid system with pumped hydro storage. Energy Convers. Manage. 111, 253–260.
Chang, T.P., 2010. Investigation on frequency distribution of global radiation using different probability density functions. Int. J. Appl. Sci. Eng. 8 (2), 99–107.
International Electrotechnical Commission., 2005. Wind turbines part 1: Design requirements. International Electrotechnical Commission. 61,400–1.
Nanda, J., Khotari, D.P., Lingamurthy, K.S., 1988. Economic- emission load dispatch through goal programming techniques. IEEE Trans. Energy Convers. 3, 26–32.
El-Keib, A., Ma, H., Hart, J., 1994. Environmentally constrained eco- nomic dispatch using the Lagrangian relaxation method. Power Syst. IEEE Trans. 9 (4), 1723–1729.
Anantasate, S., Bhasaputra, P., 2011. A multi-objective bees algorithm for multi-objective optimal power flow problem, Electrical Power Engineering and Power System. The 8th Electrical Engineering/Electronics, Computer, Telecommunications and Information Technology (ECTI) Association of Thailand-Conference.
Chen, S.D., Chen, J.F., 2003. A direct Newton-Raphson economic emission dispatch. Int. J. Electr. Power Energy Syst. 25 (5), 411–417.
Ganjefar, S., Tofighi, M., 2011. Dynamic economic dispatch solution using an improved genetic algorithm with non-stationary penalty functions. Eur. Trans. Electrical Power 21 (3), 1480–1492.
Abdullah, M.N., Bakar, A.H.A., Rahim, N.A., Moklis, H., 2013. Economic load dispatch with nonsmooth cost functions using evolutionary particle swarm optimization. IEEJ Trans. Electric. Electron. Eng. 8 (S1), S30–S37.
Peng, C., Sun, H., Guo, J., Liu, G., 2012. Dynamic economic dispatch for wind-thermal power system using a novel bi-population chaotic differential evolution algorithm. Int. J. Electrical Power Energy Syst. 42 (1), 119–126.

Karakonstantis, I., Vlachos, A., 2018. Hybrid ant colony optimization for continuous domains for solving emission and economic dispatch problems. J. Inf. Optim. Sci. 39, 651–671.
Hota, P.K., Barisal, A.K., Chakrabarti, R., 2010. Economic emission load dispatch through fuzzy based bacterial foraging algorithm. Int. J. Electric. Power Energy Syst. 32, 794–803.
Hassanien, A.E., Rizk-Allah, R.M., Elhoseny, M. 2018. A hybrid crow search algorithm based on rough searching scheme for solving engineering optimization problems, J. Ambient Intell. Hum. Comput. pp. 1–25, doi: 10.1007/s12652-018-0924-y.
Adaryani, M.R., Karami, A., 2013. 'Artificial bee colony algorithm for solving multi-objective optimal power flow problem'. Int. J. Elect. Power Energy Syst. 53, 219–230.
Harifi, S., Mohammadzadeh, J., Khalilian, M., Ebrahimnejad, S. 2020. Giza pyramids construction: An ancient-inspired metaheuristic algorithm for optimization. Evol. Intell. pp. 1–9, doi: 10.1007/s12065-020-00451-3.
Yang, X.S. 2012. 'Flower pollination algorithm for global optimization, in Unconventional Computation and Natural Computation (Lecture Notes in Computer Science), vol. 7445, J. Durand-Lose and N. Jonoska, Eds. Berlin, Germany: Springer, 2012, pp. 240–249, doi: 10.1007/978-3-642-32894-7_27.
Yao, F., Dong, Z.Y., Meng, K., Xu, Z., Iu, H.H.C., Wong, K.P., 2012. Quantum-inspired particle swarm optimization for power system operations considering wind power uncertainty and carbon tax in Australia. IEEE Trans. Ind. Inf. 8 (4), 880–888.
Cheng, R., Jin, Y., 2014. A competitive swarm optimizer for large scale. IEEE Trans. 45 (2), 191–204.
Biswas, P.P., Suganthan, P.N., Amaratunga, G.A., 2017. Optimal power flow solutions incorporating stochastic wind and solar power. Energy Convers. Manage. 148, 1194–1207.
Alsac, O., Stott, B., 1974. Optimal load flow with steady-state security. IEEE Trans. Power Apparatus Syst., 745–751
Chen, C., Lee, T., Jan, R.M., 2006. Optimal wind-thermal coordination dispatch in isolated power systems with large integration of wind capacity. Energy Convers. Manage. 47 (18), 3456–3472.
Panda, A., Tripathy, M., 2015. Security constrained optimal power flow solution of wind-thermal generation system using modified bacteria foraging algorithm. Energy 93, 816–827.
Shi, L., Wang, C., Yao, L., Ni, Y., Bazargan, M., 2012. Optimal power flow solution incorporating wind power. IEEE Syst. J. 6 (2), 233–241.
Mohapatra, P., Das, K.N., Roy, S., Kumar, R., Kumar, A., 2019. CSO technique for solving the economic dispatch problem considering the environmental constraints. Asian J. Water Environ. Pollut. 16 (2), 43–50.
Liang, J.J., Qin, A., Suganthan, P.N., Baskar, S., 2006. Comprehensive learning particle swarm optimizer for global optimization of multimodal functions. IEEE Trans. Evolut. Comput. 10 (3), 281–295.
Liang, J.J., Suganthan, P.N., 2005. Dynamic multi-swarm particle swarm optimizer. Proc. IEEE Swarm Intell. Symp., 124–129
LaTorre, A., Muelas, S., Pena, J.M., 2015. comprehensive large 316, 517–549.
Mishra, U., Wu, J.-Z., Sarkar, B., 2020. A sustainable production-inventory model for a controllable carbon emissions rate under shortages. J. Cleaner Prod. https://doi.org/10.1016/j.jclepro.2020.120268.
Roy, P.K., Ghoshal, S.P., Thakur, S.S., 2010. Combined economic and emission dispatch problems using biogeography based optimization. Electric. Eng. 92 (4–5), 173–184.
Wolpert, D.H., Macready, W.G., 1997. No free lunch theorems for optimization. Evolut. Comput. IEEE Trans. 1, 67–82.